Geol. Mag. **143** (*6*), *2006, pp. 859–876.* © *2006 Cambridge University Press*
doi:10.1017/S0016756806002585 *Printed in the United Kingdom*

Exhumation of high-pressure rocks under continuous compression: a working hypothesis for the southern Hellenides (central Crete, Greece)

V. CHATZARAS, P. XYPOLIAS* & T. DOUTSOS

Department of Geology, University of Patras, GR-26500, Patras, Greece

(*Received* 8 August 2005; *accepted* 1 March 2006)

Abstract – Combined kinematic, structural and palaeostress (calcite twinning, fault-slip data) analyses are used to study the exhumation mechanism of the high-pressure rocks exposed on the island of Crete (southern Aegean, Greece). Our study shows that the evolution of windows in central Crete was controlled by two main contractional phases of deformation. The first phase (D_1) was related to the ductile-stage of exhumation. NNW–SSE compression during D_1 caused layer- and transport-parallel shortening in the upper thrust sheets, resulting in nappe stacking via low-angle thrusting. Synchronously, intracontinental subduction led to high-pressure metamorphism which, however, did not affect the most external parts of the southern Hellenides. Subsequent upward ductile extrusion of high-pressure rocks was characterized by both down-section increase of strain and up-section increase of the pure shear component. The second phase (D_2) was associated with the brittle-stage of exhumation. D_2 was governed by NNE–SSW compression and involved conspicuous thrust-related folding, considerable tectonic imbrication and formation of a Middle Miocene basin. The major D_2-related Psiloritis Thrust cross-cuts the entire nappe pile, and its trajectory partially follows and reworks the D_1-related contact between upper and lower (high-pressure) tectonic units. Eduction and doming of the Talea Window was accompanied by gravity sliding of the upper thrust sheets and by out-of-the-syncline thrusting. Late-orogenic collapse also contributed to the exhumation process. Therefore, it seems that the high-pressure rocks of central Crete were exhumed under continuous compression and that the role of extension was previously overestimated.

Keywords: compression tectonics, high-pressure metamorphism, exhumation, Hellenides, Crete.

1. Introduction

The exhumation mechanism of high-pressure metamorphic rocks is still a crucial and debated problem, despite the numerous studies published over the decades (e.g. Platt, 1993; Fig. 1). The problem of exhumation has been well approached in Alpine-type collisional orogens (Ernst, 2005). During the main stage of the evolution of such orogens, the exhuming high-pressure rock sequences are often modelled to represent a tectonic slice bounded by a lower subduction-related thrust fault and an upper crustal-scale normal-sense fault (e.g. Chemenda, Matte & Sokolov, 1997; Ernst, Maruyama & Wallis, 1997; Vannay & Grasemann, 2001; Fig. 1b, e, f, g). It is well documented that the upper fault can represent either (a) a 'true' extensional detachment (Fig. 1b) where the high-pressure rocks are exhumed along it due to syn-orogenic crustal-scale extension (e.g. Ring *et al*. 1999; Jolivet *et al*. 2003) or (b) a 'normal fault' operating in a tectonic setting without any net extension (Fig. 1e, f). In the latter case, the high-pressure rocks in the footwall of the fault escape towards the surface under a mechanism of solid-state ductile extrusion (Fig. 1e) or buoyancy-triggered exhumation (Fig. 1f) or a combination of both (e.g. Chemenda, Matte & Sokolov, 1997; Escher & Beaumont, 1997; Vannay & Grasemann, 2001; Xypolias, Kokkalas & Skourlis, 2003). Post-orogenic extensional movements or continuous compression, which results in forward and/or backward shearing, can characterize the late-stage evolution of collisional orogens (Platt, 1993; Beaumont, Ellis & Pfiffner, 1999).

In the External Hellenides, some of the youngest high-pressure/low-temperature rocks (Early Miocene) in the world are exposed (e.g. Katagas, 1980; Fig. 2a). They are overlain by a stack of thrust sheets which show evidence of very low-grade metamorphism at the base. This metamorphic break led to various tectonic models for the island of Crete (Fig. 2b), suggesting that the contact between the high-pressure rocks and the overlying thrust sheets is a shallow-dipping extensional detachment, which formed subparallel to a subjacent subduction thrust in the Early Miocene (e.g. Kilias, Fassoulas & Mountrakis, 1994; Jolivet *et al*. 1996; Ring & Reischmann, 2002). In this case, the exhumation-related deformation was strongly localized along the extensional detachment, which is characterized by very large displacement (~ 100 km: Ring & Reischmann, 2002) contributing to the exhumation of high-pressure rocks. On the contrary, models for the

* Author for correspondence: p.xypolias@upatras.gr

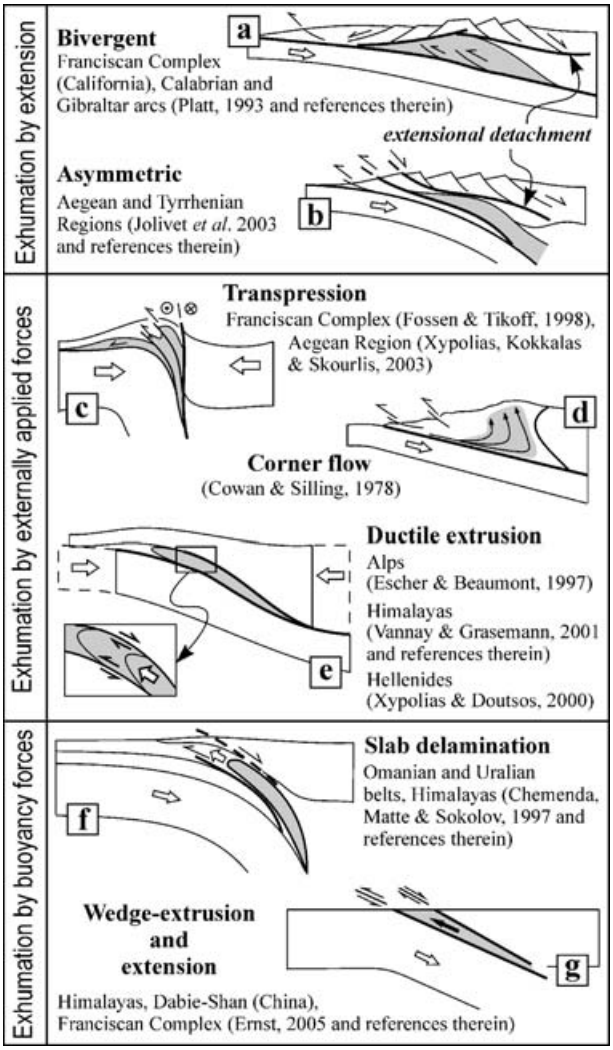

Figure 1. Summary of the most important proposed models for the exhumation mechanism of high-pressure metamorphic rocks. The various models are categorized following Platt (1993). For each model, key natural examples are provided. Grey shaded areas correspond to the exhumed high-pressure rocks.

Peloponnese suggest that exhumation was achieved by a mechanism of compressional solid-state extrusion, where the exhumed high-pressure rocks are subjected to penetrative and strongly heterogeneous ductile deformation (e.g. Xypolias & Doutsos, 2000; Doutsos *et al*. 2000).

Recent studies in Crete demonstrate that normal faulting is strongly overestimated in the orogenic evolution of the southern Hellenides (e.g. Kokkalas & Doutsos, 2001, 2004; Zulauf *et al*. 2002; Campbell, Craddock & Klein, 2003). Moreover, it is noteworthy that the proposed model suggesting major crustal extension on Crete appears to underestimate the importance of a late-orogenic contractional phase leading to the formation of asymmetric megafolds throughout the island (e.g. Wachendorf, Best & Gwosdz, 1975; Greiling, 1982; Meulenkamp *et al*. 1988). As is emphasized by many authors (e.g. Alsop, Bryson & Hutton, 2001; Bucher *et al*. 2003), restoration of the late-stage structure is a prerequisite for unravelling the main-stage orogenic evolution. In this study, we present new structural and palaeostress data from central Crete focusing especially on the geometry and kinematics of late-stage deformation. This has led us to propose an orogenic model for the Hellenides in Crete, resembling that proposed for the Peloponnese.

2. Geological framework

The Hellenides are part of the Alpine orogenic belt and form an orocline connecting the Dinarides to the north with the Taurides to the southeast (Fig. 2a). The External Hellenides are separated from the Internal Hellenides by the Pindos ophiolitic suture zone (Smith, Woodcock & Naylor, 1979), which can be traced over a distance of 1000 km from northwestern Greece through the Peloponnese to the Cretan Sea (Fig. 2a). The External Hellenides expose a pile of thrust sheets or nappes, which are traditionally referred to as units. These units consist of Upper Palaeozoic–Cenozoic sedimentary rocks that were originally deposited on top of the northern rifted margin of the Apulia microcontinent bordering the Pindos Ocean (Robertson *et al*. 1991). Nappe stacking took place from Eocene to Early Miocene times, following the closure of the Pindos Ocean and subsequent northward subduction and collision of the Apulia with several European microplates (e.g. Dewey *et al*. 1973; Doutsos *et al*. 1993).

2.a. Tectonostratigraphy

The nappe pile of Crete can be divided into two main unit/nappe groups (e.g. Seidel, Kreuzer & Harre, 1982): (a) the lower group, composed of the Plattenkalk and the Phyllite–Quartzite units which reveal Early Miocene high-pressure metamorphism and (b) the upper group, comprising in ascending order the Tripolitsa, the Pindos and the Uppermost units lacking this metamorphism (Figs 2b, 3). In central Crete, the high-pressure rocks crop out in the core of two windows, called hereafter the 'Talea' and 'Psiloritis' windows (Fig. 2b: A–A′). The entire pile of upper tectonic units is exposed on the flanks of these windows.

The para-autochthonous Plattenkalk unit represents the deepest and most external part of the Hellenides in Crete. It comprises an Upper Carboniferous to Eocene sequence of carbonate rocks (Bonneau, 1973; Krahl *et al*. 1988; Fig. 3) overlain by a Middle Oligocene flysch sequence (Bizon *et al*. 1976). Metamorphic index minerals in the Plattenkalk unit have only been found at the Talea Window and indicate *P–T* conditions of 7–10 kbar and ~350 °C (Theye, Seidel & Vidal, 1992). On the whole island, the temperature of metamorphism in the Plattenkalk unit remains nearly constant in an east–west direction, but systematically decreases from north to south (Soujon & Jacobshagen, 2001). The

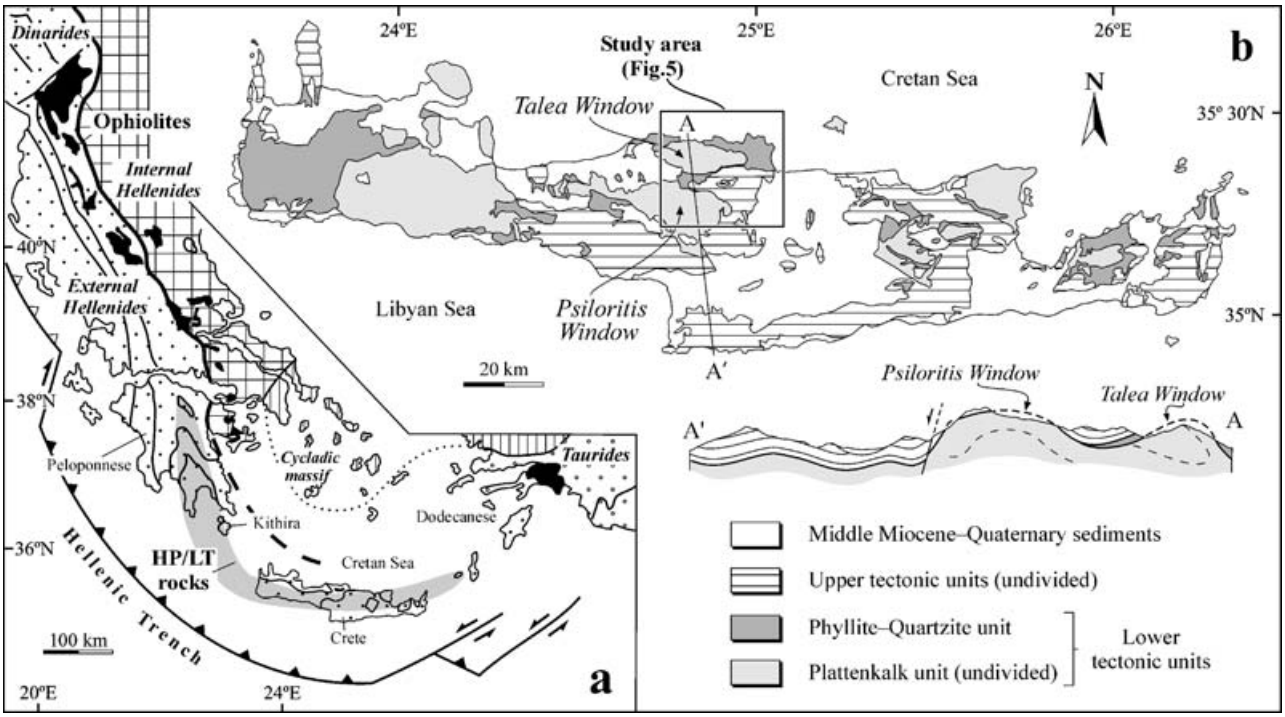

Figure 2. (a) Simplified geological map showing the position of the External Hellenides in relation to the Dinaric–Tauric arc. Grey shaded area corresponds to the exposures of high-pressure/low-temperature rocks within the External Hellenides. (b) Geological map of Crete (after Creutzburg *et al.* 1977). The structural profile A–A′ shows the Talea and Psiloritis windows and stacking of tectonic units in central Crete (after Bonneau, 1973).

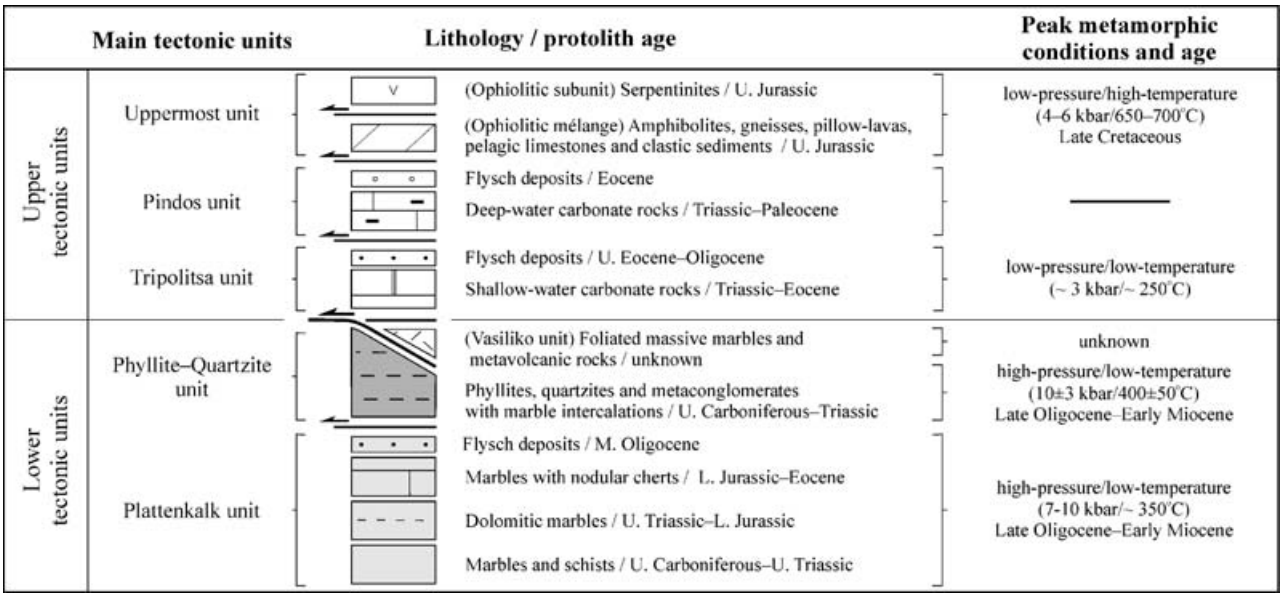

Figure 3. Tectonostratigraphic sequence (not to scale), lithologies, protolith ages, peak metamorphic conditions and metamorphic ages of the rock units in central Crete. The stratigraphic data are from Bonneau (1973, 1984), Bizon *et al.* (1976), Kopp & Ott (1977) and Krahl *et al*. (1983, 1988). Metamorphic conditions and ages are derived from Seidel, Kreuzer & Harre (1982), Feldhoff, Lücke & Richter (1991), Theye, Seidel & Vidal (1992) and Koepke, Seidel & Kreuzer (2002).

Plattenkalk unit is overridden by the allochthonous Phyllite–Quartzite unit, which represents an Upper Carboniferous to Triassic metasedimentary rift sequence (Krahl *et al*. 1983; Fig. 3). The latter shows evidence of widespread high-pressure metamorphism (Theye & Seidel, 1991; Fig. 4a). Several relic slices of pre-Alpine crystalline rocks have been identified within it, especially in Crete (e.g. Romano, Dörr & Zulauf, 2004) and recently in Kithira (Xypolias, Dörr & Zulauf, 2006). In the study area, the Vasiliko unit (Fig. 3), which

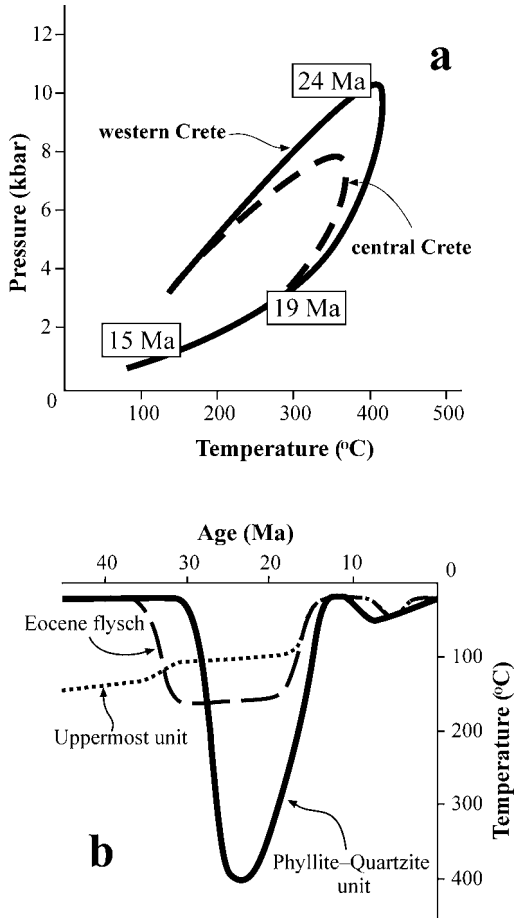

Figure 4. (a) Pressure–temperature–time (*P–T–t*) paths of the Phyllite–Quartzite unit of central and western Crete. Timing of high-pressure/low-temperature metamorphism after Seidel, Kreuzer & Harre (1982); all other age data after Thomson *et al.* (1998*a*). (b) Combined temperature–time (*T–t*) diagrams of the Phyllite–Quartzite unit, the Uppermost unit and the Eocene flysch of Crete (after Thomson *et al.* 1998*a*,*b*).

lies tectonically above the Phyllite–Quartzite unit, has not been dated up to now, but a possible pre-Alpine age for it could not be excluded (G. Zulauf, pers. comm. 2004).

The Tripolitsa and the Pindos units mainly comprise Mesozoic carbonate rocks, covered by Eocene–Oligocene flysch deposits (Kopp & Ott, 1977; Bonneau, 1984; Fig. 3). The Tripolitsa unit lies above the high-pressure units and shows evidence for very low-grade metamorphism (e.g. Feldhoff, Lücke & Richter, 1991; Fig. 3). It is noteworthy that south of the Talea Window, the Phyllite–Quartzite unit is totally absent and consequently the Tripolitsa unit lies directly above the Plattenkalk unit (Fig. 2b: A–A′). The Uppermost unit is composed of an ophiolitic subunit on top and a mélange at the base (Bonneau, 1984; Fig. 3). An Upper Jurassic age (*c.* 150 Ma) has been estimated for Cretan ophiolites, which are considered to be the southernmost outliers of the ophiolitic suture zone exposed in continental Greece (Koepke, Seidel & Kreuzer, 2002).

Unconformably above the Cretan nappe pile lies a Neogene sedimentary succession. Sedimentation in Crete starts with terrigenous sediments of Middle Miocene age, followed by Upper Miocene–Pleistocene fluviolacustrine and open-marine sediments. The stratigraphy of the Neogene is well depicted in earlier works of Fortuin (1978) and Postma, Fortuin & Van Wamel (1993).

2.b. Tectonic and thermal evolution

The tectonic evolution of the southern Hellenides began in the Eocene with a general S-directed thrusting that led to the formation of the upper tectonic units stack (e.g. Bonneau, 1984). Throughout the Oligocene, thrusting progressed towards the south as indicated by the younging trend of flysch deposits. The Middle Oligocene flysch of the Plattenkalk unit possibly marks the N-directed subduction of the Plattenkalk and the Phyllite–Quartzite units below the basement of the Tripolitsa unit. The Phyllite–Quartzite unit, which was lying northward from the Plattenkalk unit before the collision (Bonneau, 1984), possibly entered the subduction channel earlier. Within this context, the lower tectonic units suffered high-pressure metamorphism. The age of the metamorphic peak is constrained at *c.* 24 Ma using K–Ar and Ar–Ar ages of white mica from the Phyllite–Quartzite unit (Seidel, Kreuzer & Harre, 1982; Jolivet *et al.* 1996). Fluid inclusions (Küster & Stöckhert, 1997) and fission-track data of zircon and apatite (Thomson *et al.* 1998*a*) from the Phyllite–Quartzite unit rocks also reveal that subsequent exhumation to a depth of $\sim$10 km and cooling to $\sim$300 °C should have been completed before 19 Ma (Fig. 4a). Final cooling of the Phyllite–Quartzite unit to about 100 °C took place at *c.* 15 Ma. Simultaneously, the upper units seem to have undergone a phase of accelerated denudation at 17–11 Ma (Fig. 4b), as suggested by apatite fission-track analysis in rocks of the Uppermost unit and the slightly heated Pindos flysch (Thomson *et al.* 1998*b*). This implies a progressive increase in topography and relief of the belt during Middle Miocene times. Finally, the presence of pebbles derived from the Plattenkalk and the Phyllite–Quartzite units, within the lower parts of the Neogene sedimentary succession in Crete which are dated by microfossils to the Middle–Late Miocene boundary (*c.* 11 Ma: Fortuin, 1978), indicate that rocks of the high-pressure units had reached the Earth's surface by that time.

3. Deformation history

Our structural survey in the area establishes the bulk geometry of the windows and unravels the successive deformation phases of the Cretan tectonic units. To better understand the deformation history, we mapped the southern part of the area at a 1:10 000 scale (Fig. 5),

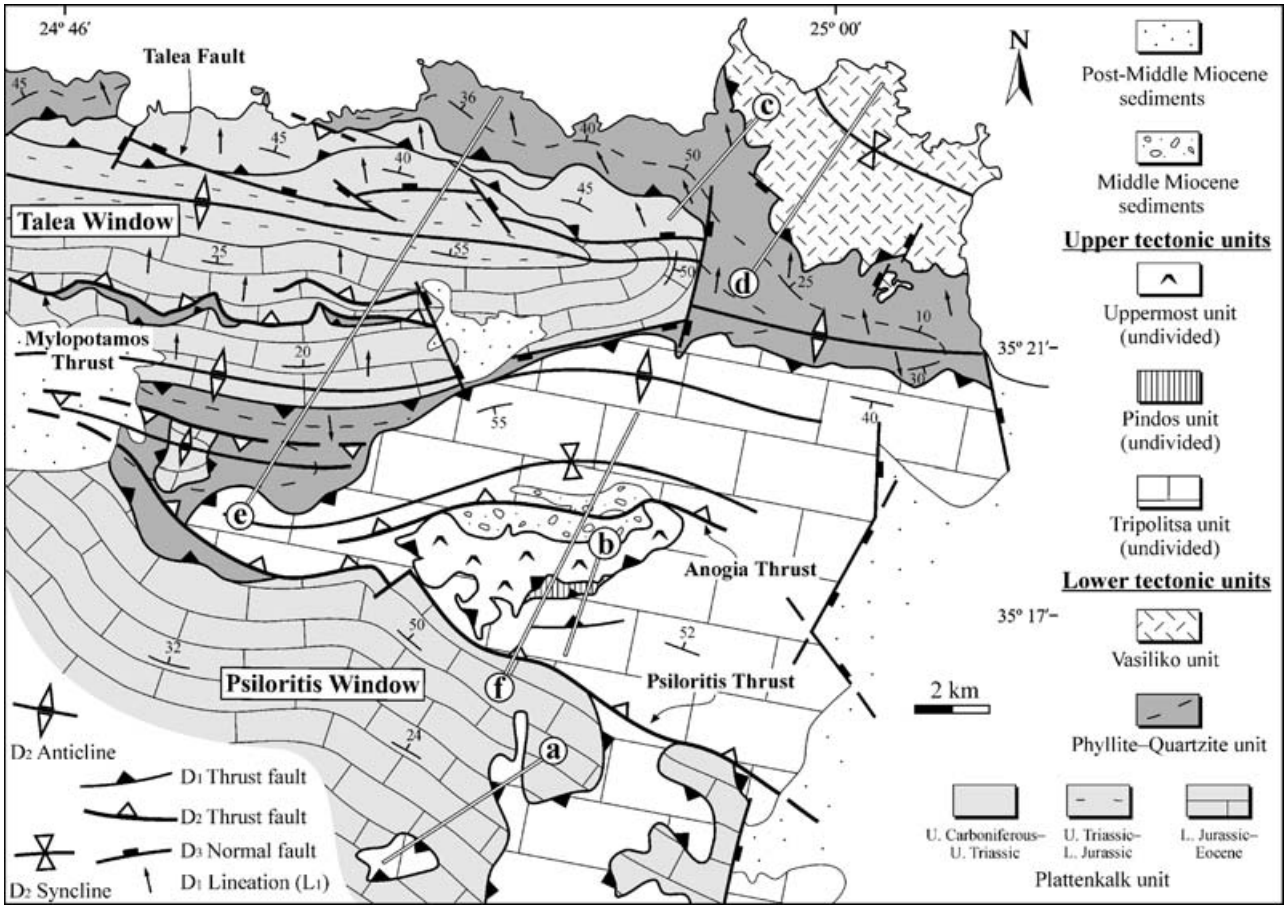

Figure 5. Structural map of the Talea Window and the northern flank of the Psiloritis Window. The location of the map is given in Figure 2b. Lettered sections a, b, c and d, e, f refer to the cross-sections in Figures 6 and 8, respectively.

augmented previous maps for the Talea Window (Epting, Kudrass & Schäfer, 1972; Hall & Audley-Charles, 1983) and carried out detailed structural analysis throughout the area. Previously, Creutzburg *et al*. (1977) mapped the entire area at a 1:200 000 scale. Based primarily on overprinting criteria observed in map to outcrop scales as well as on microstructural data, we have distinguished three principal deformation phases (D_1–D_3) to constrain the evolution of the thrust belt. The first phase (D_1) involves brittle and ductile deformation in the upper and lower tectonic units, respectively. Low-angle D_1 thrusting and related structures resulted in the formation of the Cretan nappe pile, including the juxtaposition of the upper with the lower tectonic units. The second semi-brittle to brittle phase (D_2) is characterized by folds and thrusts, which have affected the whole nappe pile. The last phase (D_3) is represented by moderate to steep normal faults.

3.a. Early contractional phase (D_1)

3.a.1. Upper tectonic units

Although the main S-directed thrusting that caused the stacking of upper thrust sheets has not been extensively described, there is no major controversy regarding this (e.g. Bonneau, 1984; Kilias, Fassoulas & Mountrakis, 1994; Kokkalas & Doutsos, 2004). Therefore, in the following we briefly summarize our findings related to the D_1 structures. The whole sequence of the upper thrust sheets is exposed at the northern flank of the Psiloritis Window (Fig. 5). There, the thickness of the Pindos unit is small, and in places the Uppermost unit is directly emplaced over the rocks of the Tripolitsa unit (Fig. 5). All structural units are bounded by N-dipping bedding-parallel D_1 thrusts (Fig. 6a, b). In the ophiolitic subunit, thrusting is accommodated by the formation of duplex structures on a decametre-scale (Fig. 7b). All the duplexes found are of hinterland-dipping type (e.g. McClay, 1992). Statistical analysis shows that the minor roof and floor thrusts intersect with the link thrusts in an ENE-trending line implying top-to-the-SSE thrusting (Fig. 6: IV). Deformation patterns within the mélange subunit and the Pindos unit are mainly characterized by asymmetric folds with roughly ENE-trending axes and N-dipping axial surfaces (Fig. 6: III and I, respectively). The intersection lineations of bedding planes and D_1-related cleavage in the Pindos unit trend parallel to the F_1 fold axes (Fig. 6: II). The Tripolitsa unit is

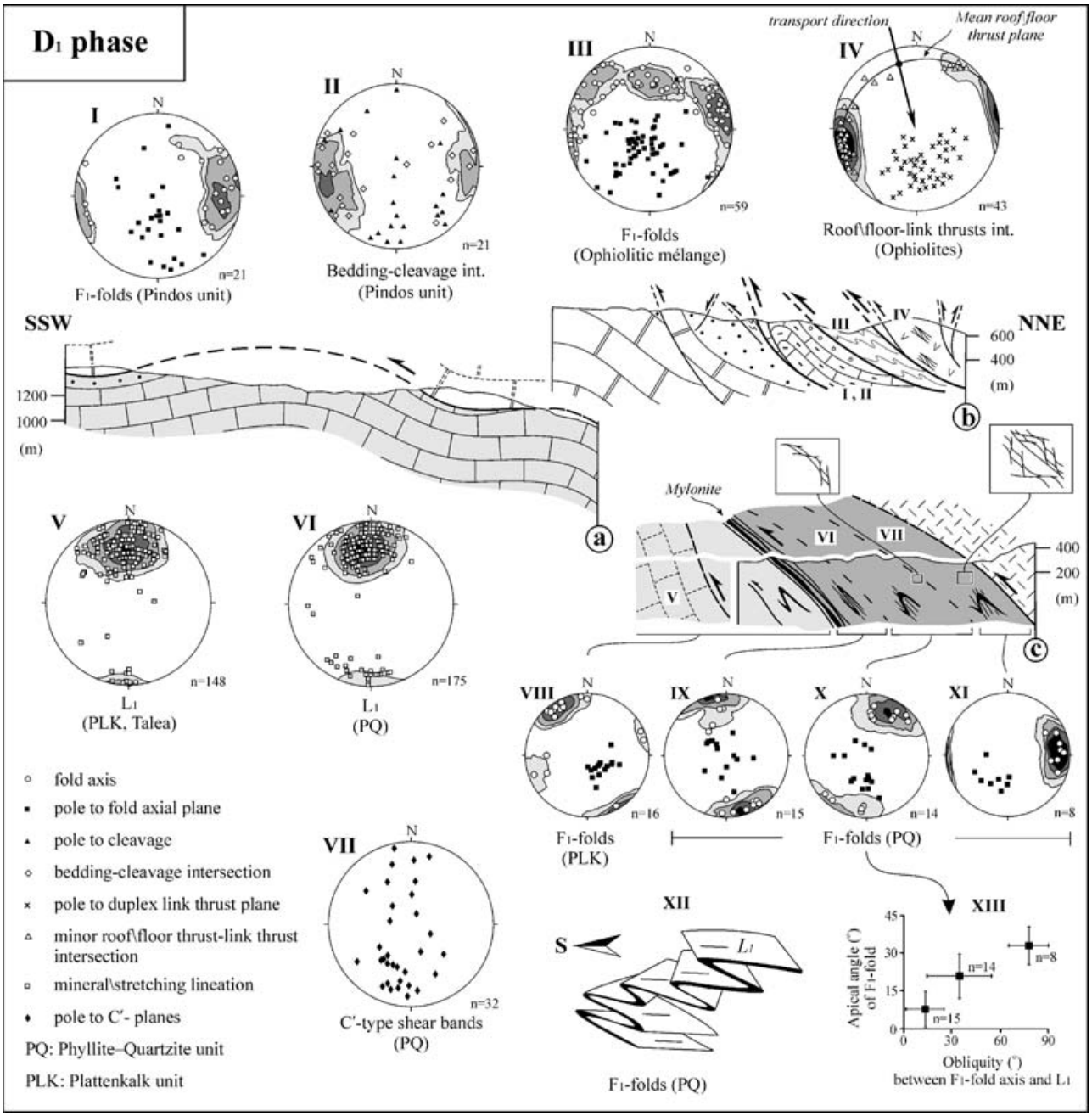

Figure 6. Cross-sections (a–c) and equal-area lower hemisphere projections (I–XI) for the D_1 phase of deformation. Ornaments as in Figure 3; locations of plots I–VII are shown on the cross-sections; locations of sections are shown in Figure 5. XII is a block sketch showing the rotation and tightening of F_1 folds towards the lower structural levels of the Phyllite–Quartzite unit. Data from folds projected at IX, X and XI are used to construct the graph XIII, illustrating the variation in apical angles of F_1 folds v. obliquity between F_1 fold axes and stretching lineation. Black squares in the graph correspond to average values of each group of folds.

internally deformed by bedding-parallel thrust faults and small-scale duplex structures, all compatible with top-to-the-SSE sense of thrusting. As a whole, our structural analysis confirms the previously suggested roughly S-directed D_1 thrusting and specifies a NNW–SSE transport direction for the upper thrust sheets. A sporadically observed E-trending mineral lineation in amphibolites of the ophiolitic mélange is defined by minerals related to Late Cretaceous high-grade metamorphism (Fig. 3; Kilias, Fassoulas & Mountrakis, 1994) and is associated with a pre-Eocene deformation event. The tectonic significance of this event remains enigmatic.

3.a.2. *Lower high-pressure tectonic units*

The main ductile deformation (here D_1) in the Phyllite–Quartzite unit is accompanied by a penetrative foliation (S_1) which post-dates the main growth of high-pressure related minerals (Theye & Seidel, 1991). Relics of

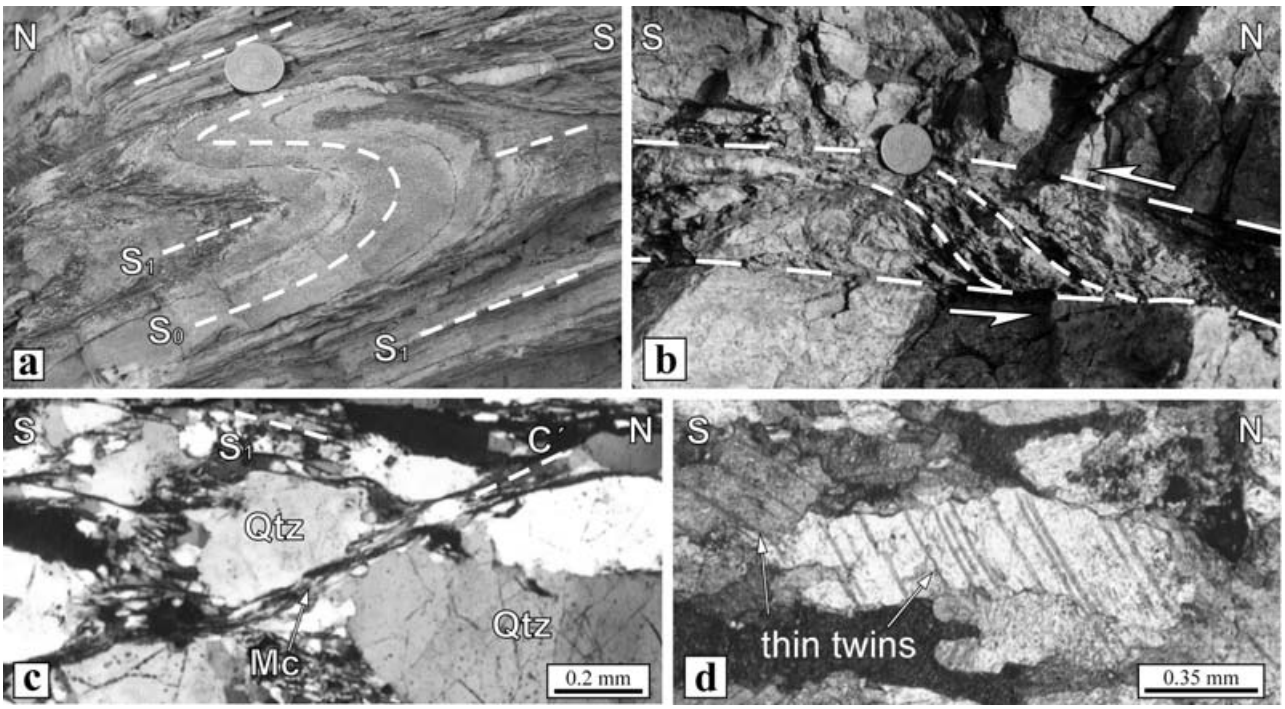

Figure 7. Mesoscopic and microscopic features of the D_1 phase in the Plattenkalk and the Phyllite–Quartzite units. (a) The main S_1 foliation is axial planar to an F_1 fold. The latter deforms S_0 bedding of the Phyllite–Quartzite unit (coin diameter is 32 mm). (b) Duplex structures and duplex link thrusts in serpentinites of the Uppermost unit indicating top-to-the-S sense of shearing (coin diameter is 34 mm). (c) Micrograph (XPL) of C′-type shear band from a sample at the upper structural levels of the Phyllite–Quartzite unit. White mica (Mc) is recrystallized along the C′ surface; Qtz – quartz. (d) Micrograph (XPL) of twinned calcite grains of the Plattenkalk unit rocks in the Psiloritis Window. Thin and straight calcite twins imply low-temperature deformation.

a pre-D_1 deformation are found in the form of an internal planar foliation in porphyroclastic high-pressure related minerals (e.g. chloritoid). The S_1 is by far the dominant structural feature observed in outcrop scale. It is typically defined by the shape-preferred orientation of mica and elongated quartz grains. Well-developed within the plane of S_1 is a NNW-trending mineral/stretching and clast-elongation lineation (L_1; Figs 5, 6: VI). The S_1 is axial planar to isoclinal minor F_1 folds. The F_1 folds are commonly tight to isoclinal (Fig. 7a), almost recumbent in style, with curvilinear hinges and fold axes oblique to sub-parallel to the L_1. Structural mapping at the northern flank of the Talea Window showed that there is a progressive decrease in both the apical angle of F_1 folds and the range of obliquity between fold axes and stretching lineation orientation towards the lower structural levels of the Phyllite–Quartzite unit (Fig. 6: IX to XIII). This finding is indicative of a progressive rotation of fold axes into the X-axis of finite strain (e.g. Alsop, 1992), resulting from an overall increase in strain magnitude as the contact between the Phyllite–Quartzite and the Plattenkalk units is approached. Asymmetrical F_1 folds with axes at a high angle to L_1 exhibit southward vergence, indicating thrusting of the Phyllite–Quartzite unit over the Plattenkalk unit. A similar top-to-the-SSE sense of movement is also confirmed by kinematic indicators such as C/S fabrics and σ-shaped objects, found within a $\sim$30 m thick mylonitic zone developed at the contact between the Phyllite–Quartzite and the Plattenkalk units in the Talea Window. A system of top down-to-the-N and top down-to-the-S C′-type shear bands (Fig. 6: VII) also occurs sporadically throughout the Phyllite–Quartzite unit, but both appear to be more frequent at the upper structural levels of the unit (Fig. 6c: insets). The two sets exhibit similar structural styles and are interpreted to be contemporaneous, indicating a component of bulk pure shear deformation (e.g. Simpson & De Paor, 1993; Law, Searle & Simpson, 2004). The finding that fine-grained white mica recrystallizes along shear band surfaces (Fig. 7c) suggests that these structures are late D_1 features.

The first deformational phase in the Plattenkalk unit produced a bedding-parallel metamorphic foliation (S_1), which contains a roughly N-trending stretching lineation (L_1; Figs 5, 6: V). The S_1 fabric is defined by the dimensional alignment of calcite grains in marbles, the preferred orientation of platy minerals in pelitic intercalations and recrystallized quartz grains in nodules of metacherts. At the mesoscopic scale, carbonate rocks of the Plattenkalk unit are deformed by isoclinal intrafolial F_1 folds with axes sub-parallel to L_1 (Fig. 6: VIII). Ductile folding of the Plattenkalk unit is especially prominent in the 20–30 m thick marble mylonite, which occurs along the contact with

the overlying Phyllite–Quartzite unit. Moreover, it is important to note that D_1 fabric elements and structures are conspicuous in the Talea Window but seem to decline or disappear in the southern part of the study area. Analyses of carbonate samples collected from the Plattenkalk unit in the Psiloritis Window show that calcite grains are largely deformed by straight type-I and/or type-II twins (Fig. 7d; see also Section 4.a), indicating a temperature below 300 °C (e.g. Burkhard, 1993). These observations imply that the metamorphism and intensity of D_1 deformation in the Plattenkalk unit decrease southwards.

In agreement with previous interpretations for eastern Crete (e.g. Zulauf *et al*. 2002; Kokkalas & Doutsos, 2004) and the Peloponnese (Doutsos *et al*. 2000), we suggest that the above-described D_1 ductile structures have been formed during the exhumation and emplacement of the Phyllite–Quartzite unit over the Plattenkalk unit. At the northern flank of the Talea Window the Phyllite–Quartzite unit is thrust over a tectonic slice, which is internally imbricated by ductile thrust faults (Figs 5, 6c). This slice consists of metamorphosed Carboniferous–Triassic carbonate and pelitic rocks (Figs 5, 6c), which are interpreted by many authors as the older part of the Plattenkalk unit (e.g. Epting, Kudrass & Schäfer, 1972; Krahl *et al*. 1988). They probably represent the lateral proximal equivalent of the Phyllite–Quartzite unit protolith. Alternatively, Hall & Audley-Charles (1983) interpreted this rock slice as part of the Phyllite–Quartzite unit. In our view, these Plattenkalk unit rocks were stripped from their basement and thrust southward during the D_1 phase (Fig. 6c). Further to the south the Phyllite–Quartzite unit overrides the upper parts of the Plattenkalk unit (Fig. 5).

3.a.3. Contact between upper and lower units

In the study area, the contact between upper and lower tectonic units is always marked by a 1–50 m thick cataclastic zone. This, in combination with the fact that thick cataclastic zones are associated with D_2 thrusts (see below), possibly indicates that early juxtaposition of upper and lower units was followed by D_2 movements in the brittle field, which reworked the contact.

3.b. Late contractional phase (D_2)

The second phase of deformation has produced well-developed structures that formed under semibrittle to brittle conditions. Meso- to map-scale folds and thrust faults, which trend roughly E–W to WNW–ESE and accommodate a top-to-the-SSW sense of shear, are the prominent D_2 structural features (Fig. 5).

3.b.1. Typical structural elements in meso-scale

All of the above-mentioned D_1 fabric elements and structures in the Phyllite–Quartzite unit are overprinted by NNE–SSW contraction-related structures (D_2). Parallel or chevron to kink folds are the dominant D_2 structures at outcrop scale occurring throughout the Phyllite–Quartzite unit. They are predominantly open to tight SSW-vergent folds, with moderately dipping axial planes, and ESE-trending sub-horizontal axes (Fig. 8: I, II). Parallel to the axial planes of F_2 folds a widely spaced cleavage (S_2) is locally developed (Fig. 9a). Corrosion of quartz and mica grains along axial planar cleavage surfaces indicates that dissolution–mass transfer processes played an important role in the formation of some F_2 folds.

D_2 deformation in the Plattenkalk unit is mainly expressed by widespread folding (F_2) of bedding-parallel foliation (S_1), and a spaced cleavage (S_2). Typically, the F_2 folds are close to tight, strongly asymmetric parallel or chevron folds (Fig. 9e) with WNW-trending axes (Fig. 8: III, V) and generally exhibit vergence towards the SSW. They are associated with only limited development of an axial planar cleavage. The limbs of F_2 folds generally maintain constant thickness and are commonly characterized by structural features (e.g. duplexes) indicating bedding-parallel movements compatible with a flexural-slip mechanism. The hinges of folds at Psiloritis are more angular than those observed northward at the Talea Window. Moreover, hinges and limbs of F_2 folds are often cut by low-angle faults with top-to-the-S transport (Fig. 9d) that are compatible with R_1-Riedel and P shear surfaces commonly described in thrust zones (Woodward *et al*. 1988). This probably indicates that folds 'locked up' and then underwent additional S-directed shearing. The S_2 cleavage is very widely spaced and developed by pressure solution with no evident associated growth of metamorphic minerals. It dips moderately–steeply to the NNE and occurs in two settings: (a) sporadically in the hinge regions and the limbs of tight F_2 folds representing an axial planar cleavage and (b) in areas without any evident outcrop-scale F_2 folds as a densely spaced NNE-dipping solution cleavage (S_{2A}; Fig. 9b). In this case, the intersection lineations of S_1 and S_{2A} (Fig. 8: IV, VI) trend parallel to the F_2 fold axes. Also, a less densely spaced SSW-dipping solution cleavage is locally developed near backthrust faults (S_{2B}; Fig. 9b).

Mesoscopic faulting and fracturing account for much of the D_2-related deformation within the upper tectonic units. However, the D_2 structures can be distinguished with certainty from D_1-related structures only close to major map-scale thrust faults described below.

3.b.2. Map-scale structures

Three major N- to NNE-dipping thrust faults (Psiloritis, Anogia and Mylopotamos thrusts; Figs 5, 8: d, e, f), which are associated with the formation of megafolds in their hanging-walls, represent the prominent second-phase structures at the map scale. These structures

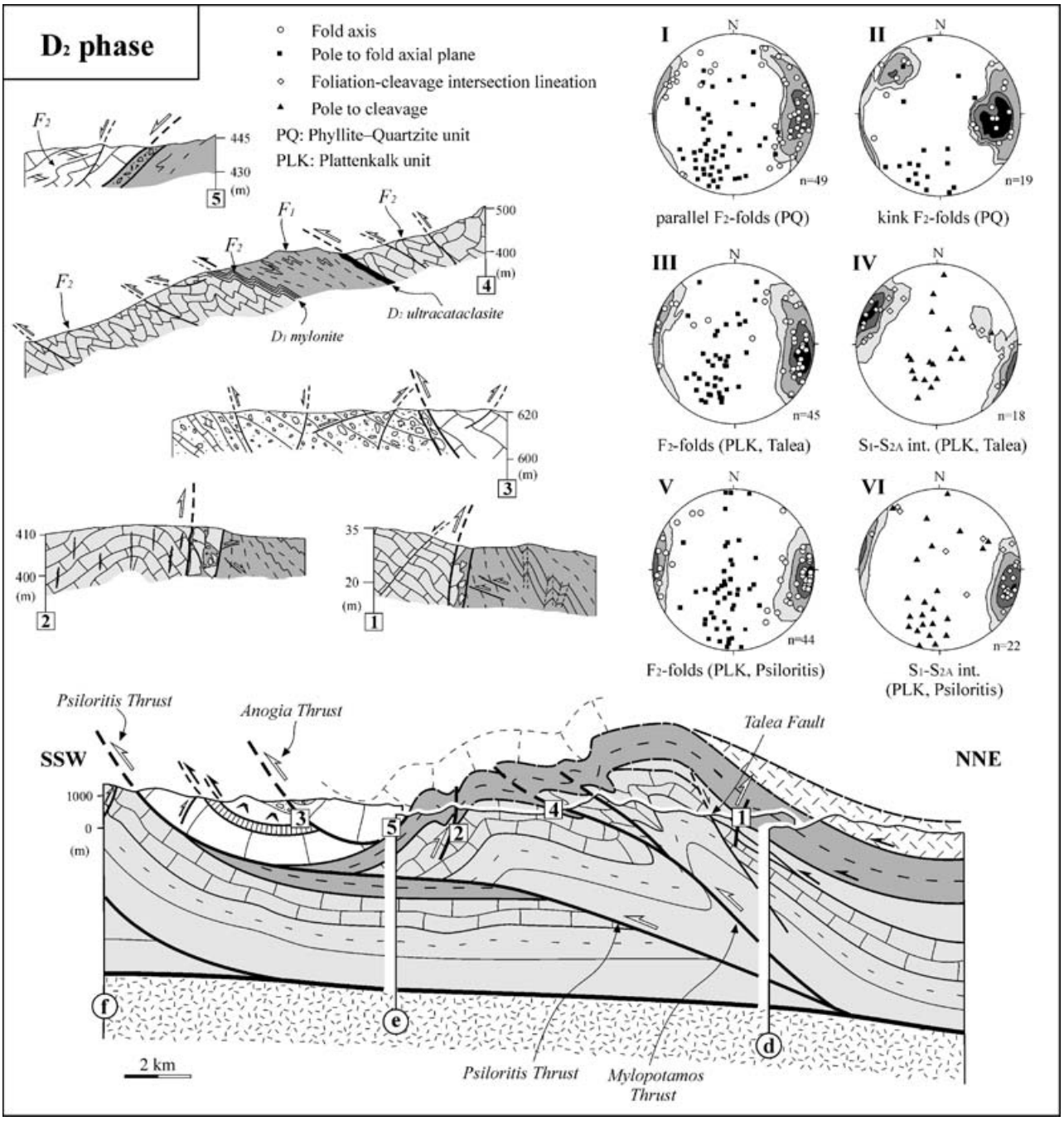

Figure 8. Cross-sections and equal-area lower hemisphere projections for the D_2 phase of deformation. For location of the composite section d–e–f, see Figure 5. Black arrows refer to D_1-related thrusts, white to D_2-related thrusts. Legend as in Figure 5.

affect the whole nappe pile in the area and deform the early map-scale thrusts (D_1). Two SSW-dipping backthrusts are also recognized at the northern and southern flanks of the Talea Window, respectively (Figs 5, 8: 1, 2). The backthrusts are accompanied by brecciation and carry the carbonate rocks of the Plattenkalk unit above the Phyllite–Quartzite unit. Backthrusts causing smaller stratigraphic separation also occur throughout the area.

The Psiloritis Thrust is exposed at the northern flank of the Psiloritis Window and extends for at least 25 km along-strike (Fig. 5). As indicated in the map, it cross-cuts the entire nappe pile, and its trace partially coincides with that inferred as an extensional detachment between lower and upper tectonic units (Fig. 5). In the central part of the thrust a 20–40 m thick cataclastic zone separates the Plattenkalk and the Tripolitsa units. In the footwall, the Plattenkalk unit is dramatically deformed by WNW-trending strongly asymmetric F_2 folds indicative of SSW-directed thrusting (Fig. 9d). In the hanging-wall, the Tripolitsa unit rocks are mainly deformed by a densely spaced, steeply dipping solution cleavage. In order to describe the subsurface structure of the Psiloritis Thrust, we extrapolated the first-order

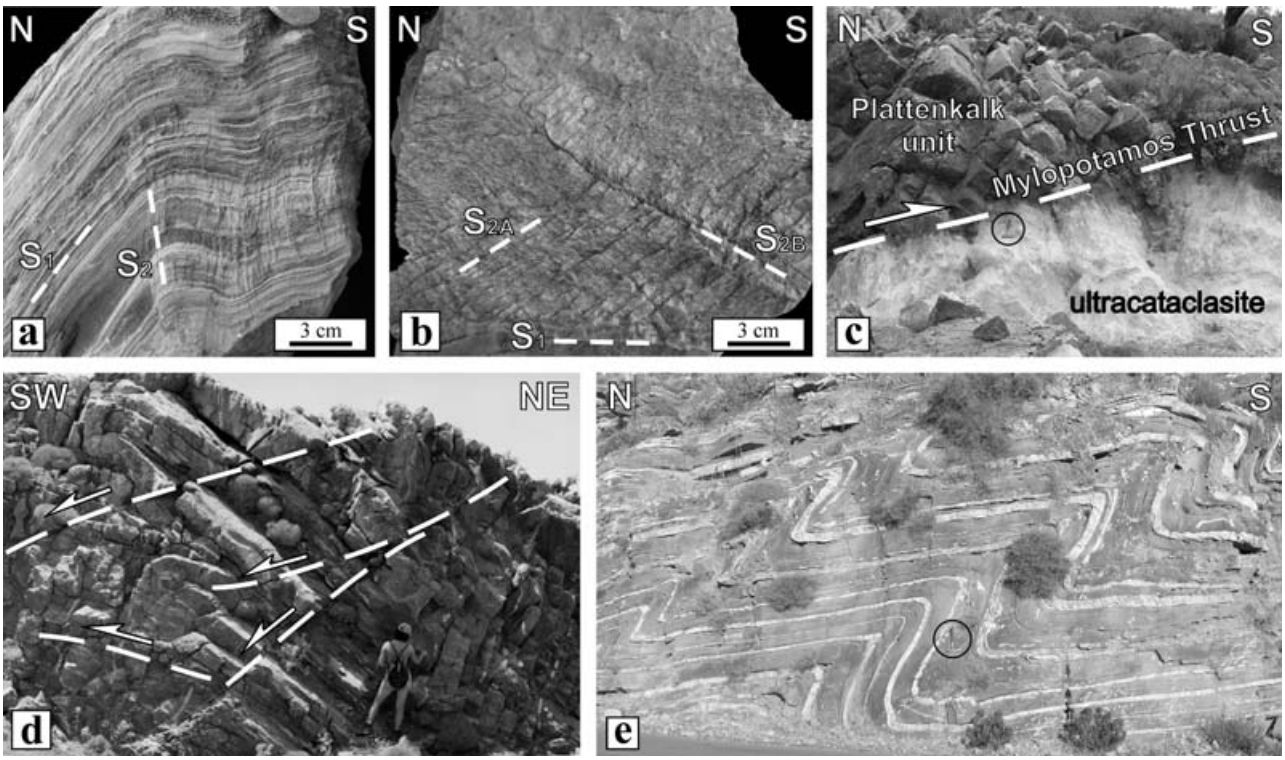

Figure 9. Mesoscopic and hand specimen features of the D_2 phase in the Plattenkalk and the Phyllite–Quartzite units. (a) F_2 fold in the Phyllite–Quartzite unit with axial planar cleavage (S_2), along which corrosion of quartz and mica grains occurred. (b) Marble specimen from the Plattenkalk unit, showing the existence of three planar fabrics. S_1 is the bedding-parallel metamorphic foliation; S_{2A} is a spaced cleavage formed during the main top-to-the-S phase of D_2 deformation and cross-cuts S_1; S_{2B} formed during top-to-the-N backthrusting (late D_2) and cross-cuts both S_1 and S_{2A}. (c) Mesoscopic view of the Mylopotamos Thrust. Along the thrust surface, a 10 m thick ultracataclasite has formed (hammer length is 32 cm). (d, e) Mesoscopic photographs of F_2 folds from the Plattenkalk unit in the Psiloritis and Talea windows, respectively (hammer length is 32 cm).

structures at depth following guidelines set out in Woodward, Boyer & Suppe (1989) for balanced cross-sections. As illustrated in Figure 8 (sections d, e, f) an upright, slightly asymmetric, S-verging anticline with high interlimb angle ($\sim 120^\circ$) occupies the hanging-wall of the Psiloritis Thrust. The anticline is cored by the Plattenkalk unit rocks and is interpreted as a fault-bend fold overlying the crest of a footwall ramp through lower tectonic units. High-angle backthrusting at the forelimb of this hanging-wall anticline is also compatible with translation of strata and folding over a blind thrust with ramp-flat geometry (e.g. Dunne & Ferrill, 1988). The flat part is developed along the pre-existing contact between upper and lower tectonic units, reworking it. The thrust probably soles out into a bedding-parallel décollement horizon located at the base of the nappe pile at a depth of around 5–6 km. This interpretation is in accordance with geophysical data from central Crete (Bohnhoff *et al*. 2001) showing that the interface between Alpine and pre-Alpine basement rocks occurs at this depth.

The Anogia Thrust (Figs 5, 8) extends for at least 11 km along strike and transports the carbonate rocks of the Tripolitsa unit southward over 100 m thick terrigenous sediments of Middle Miocene age (Serravallian: van Hinsbergen & Meulenkamp, 2006). The thrust fault zone is marked by 5–10 m thick cataclasites and limestone breccias. The Middle Miocene sediments fill a narrow basin (Fig. 5) and largely consist of matrix-supported conglomerates, sandstones and a thin marl horizon on top. Boulders of fault-derived breccias covered by marl layers were found close to the thrust, suggesting that the hanging-wall uplift took place during sedimentation. Intra-basinal deformation is mainly expressed with S- and N-directed reverse faults (Fig. 8: 3). Few asymmetric S-verging folds are identified within the upper marl horizon. We interpret the Anogia Thrust as an out-of-the-syncline thrust (in the sense of McClay, 1992) which was developed at the leading hanging-wall syncline of the Psiloritis Thrust (Fig. 8: d, e, f). It probably soles out at the base of upper tectonic units along the ~ 5 m thick cataclastic zone defining the contact between the Tripolitsa and the Phyllite–Quartzite units. Above the cataclastic zone, the Tripolitsa unit rocks are deformed by recumbent folds (F_2), which are genetically related to normal faults indicating S-directed sliding (Fig. 8: 5).

The Mylopotamos Thrust (also mapped by Hall & Audley-Charles, 1983) can be traced for about 10 km in the core of the Talea Window (Figs 5, 8). In the

hanging-wall of the Mylopotamos Thrust a minor thrust segment, which represents a splay of a larger structure and an ESE-trending map-scale anticline, were also mapped. The hanging-wall anticline is characterized by an overturned N-dipping forelimb and a moderately dipping backlimb showing clear S-vergence. The fault zone of the Mylopotamos Thrust consists of a 10 m thick ultracataclasite (Fig. 9c) along which the carbonate rocks of the Plattenkalk unit thrust over quartzites and phyllites of the Phyllite–Quartzite unit. The zone of ultracataclasite is bounded by a broad zone where the rocks of both Plattenkalk and Phyllite–Quartzite units are dramatically deformed into tight to isoclinal S-verging F_2 folds (Fig. 8: 4). Within this zone the forelimbs of folds are cut by several minor N-dipping thrusts, which are associated with brecciation and frequently disrupt the structure. Intense F_2 folding has also affected the mylonitic zone defining the thrust contact (D_1) between the Plattenkalk and the Phyllite–Quartzite units. The observed localization of F_2 folds near the Mylopotamos Thrust and various minor thrust faults suggest a genetic link between faulting and fold development. However, faulting and cataclastic deformation probably began during the later stages of D_2 folding. On the basis of this finding we interpret the whole structure in the core of the Talea Window as a complex thrust-propagation fold developed during the D_2 phase. By analogy with other natural examples, we suggest that the sequential evolution of this structure probably involves blockage of fold growth and subsequent up-dip propagation of a thrust fault, which finally breaks through the fold and obscures the original shape (e.g. Suppe & Medwedeff, 1990; Erslev & Mayborn, 1997).

3.c. Extensional phase (D_3)

D_3 is an entirely brittle phase, associated with the formation of post-Middle Miocene basins. It includes two sets of high-angle normal faults, which strike WNW–ESE and NNE to NNW, respectively. The map pattern (Fig. 5) indicates that the second set is the latest. Both sets cross-cut the entire nappe pile and overprint all previous structures. As indicated in Figure 8, sections d and e, a major WNW-striking D_3 fault (Talea Fault) cuts the northern limb of the anticline occupying the core of the Talea Window. Normal faults of the second set possibly have an oblique component of displacement that is indicated by the offset and curvature of older structures along these on the map view. A thorough description of this phase is given in Kokkalas & Doutsos (2001).

4. Stress analysis

Stress analysis was carried out to decipher further the complicated and controversial tectonic evolution of the contact between upper and lower nappes. We focus our analysis mainly at the northern flank of the Psiloritis Window, where the contact partially coincides with the Psiloritis Thrust (Fig. 10). Calcite twinning analysis was performed in order to record the strain and derive the stress field. The latter was also derived from fault-slip data analyses.

4.a. Sampling and methods

Eight oriented samples of wackestone and packstone were collected from the Plattenkalk ($n = 3$) and the Tripolitsa ($n = 5$) units (Table 1) for calcite twinning analysis. Sampling was carried out along a ~ 10 km long traverse running perpendicular to the mean structural trend. Six samples were situated near the Psiloritis Thrust and two were positioned in the hanging-wall block of the Anogia Thrust (Fig. 10). All samples were collected away from zones of intense local deformation (e.g. fold hinges), in order to reflect regional strain patterns. Calcite grains contain type-I and type-II twins (Burkhard, 1993) with widths ranging between 0.2 and 4 μm, implying deformation temperature below 300 °C for both the Plattenkalk and the Tripolitsa units. Calcite twinning analysis involved (a) Turner's (1953) dynamic analysis which was used to obtain the orientations of principal stress axes and (b) Groshong's (1972) strain gauge technique for calculation of strain responsible for twinning. At least 25 grains from each of two mutually perpendicular thin-sections were measured. The resultant data were analysed using the calcite strain-gauge program of Evans & Groshong (1994), which calculates the complete stress/strain tensor. The program computes the positive (PEVs) and negative (NEVs) expected values for the analysed twins of a given sample. PEVs and NEVs represent grains that were favourably and unfavourably oriented for twinning in the determined stress field, respectively. Adopting Teufel (1980), PEVs and NEVs were analysed separately in order to test for discrete deformation events. Both analyses should yield percentages of newly calculated NEVs smaller than the threshold value of 15 % (according to Teufel, 1980) so as to accept their results as robust. In our samples, these percentages are satisfactorily low for the PEVs but they exceed the threshold value for the initial NEVs. Therefore, we accept as robust the results of the PEVs analyses only (Table 1).

Fault-slip data were selected from all structural units exposed near the Psiloritis Thrust as well as from Middle Miocene sediments (Fig. 10). Data correspond to measurements of striations and other sense-of-slip indicators on map to outcrop scale faults, determined using criteria summarized by Hancock (1985). In total, data for 85 faults were selected from six locations and were analysed using the Tensor program (Delvaux, 1993). Application of the optimization method provided by the program discarded around 30 % of the original dataset. The remaining data were

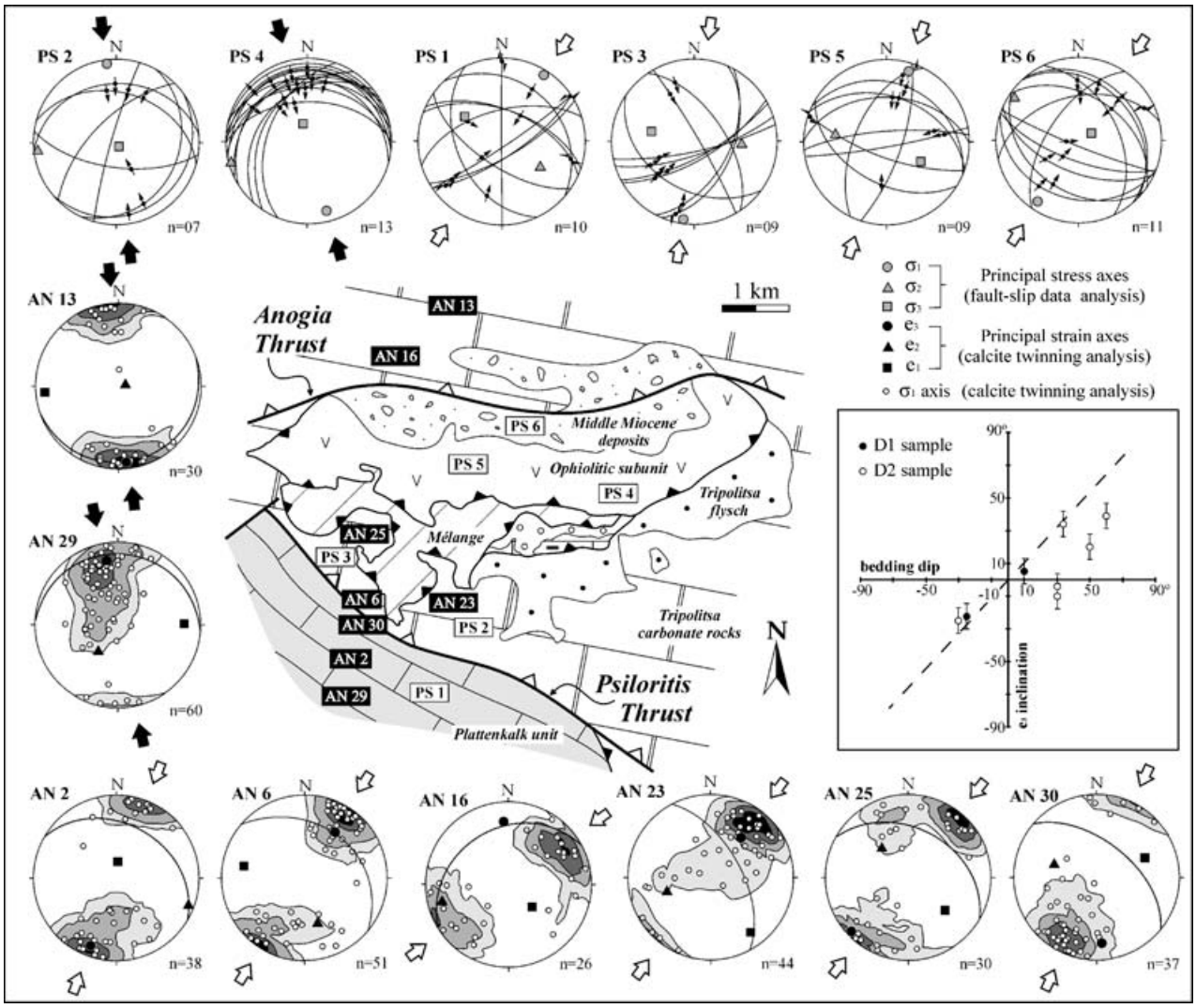

Figure 10. Lower hemisphere equal-area projections of calcite twinning and fault-slip data analysis results. In the stereoplots of fault-slip data results, only the data producing the best-fitting tensors are presented. Stereoplots of calcite twinning analysis contain the principal strain axes as well as contoured compressive stress axes calculated with Groshong's (1972) strain gauge technique. Sampling sites for calcite twinning analysis and sites of fault-slip data collection are plotted on the geological map from the northern flank of the Psiloritis Window. Black triangles on map refer to D_1-related thrusts and white to D_2-related thrusts. Ornaments as in Figure 3. Inset: maximum shortening (e_3) axes dip v. bedding dip plot. Dashed line refers to values of equal e_3-axes plunge and bedding dip while error bars are $\pm 8^\circ$ (Groshong, Teufel & Gasteiger, 1984).

Table 1. Calcite twinning analysis results

		PEVs		Strain orientations (percent elongation)			Stress		
Sample	Tectonic unit	M/N	S.E.	e_3	e_2	e_1	σ_1 (C)	σ_3 (T)	Bedding
AN 2	Plattenkalk	38/0	0.143	200/15 (−0.315)	109/04 (−0.044)	005/74 (0.359)	201/06	135/70	030/30
AN 6	Tripolitsa	56/5	0.509	031/34 (−1.511)	161/43 (−0.039)	281/27 (1.550)	032/15	281/10	032/34
AN 13	Tripolitsa	33/3	0.943	175/02 (−2.221)	069/83 (0.316)	265/07 (1.905)	176/06	330/80	160/10
AN 16	Tripolitsa	30/4	0.998	355/25 (−2.928)	256/19 (0.398)	134/58 (2.530)	054/30	204/65	330/30
AN 23	Tripolitsa	45/1	0.769	038/40 (−4.631)	253/44 (0.082)	144/19 (4.550)	027/12	154/55	062/60
AN 25	Tripolitsa	31/1	0.811	225/04 (−2.188)	320/50 (0.095)	131/40 (2.093)	034/06	153/45	030/30
AN 29	Plattenkalk	68/8	0.746	358/22 (−1.772)	226/58 (−0.322)	097/21 (2.094)	348/30	133/45	011/25
AN 30	Plattenkalk	44/7	0.124	175/21 (−0.283)	288/45 (0.092)	069/37 (0.191)	205/18	040/75	045/50

PEVs–population of positive expected values obtained from the analysis of raw data; M–number of twin sets analysed; N–number of associated NEVs; S.E.–standard error; e_3, e_2, e_1–orientations (azimuth and plunge) and percent elongations (negative values indicate shortening) of principal strain axes; σ_1, σ_3–orientations of Turner's (1953) dynamic analysis compression (C) and tension (T) stress axes, respectively.

Table 2. Palaeostress tensors from fault-slip data analysis

Site	Tectonic unit	n	σ_1	σ_2	σ_3	R	A	Stress regime
PS 1	Plattenkalk	10	033/01	123/44	303/46	0.1	7.5	Compressive
PS 2	Tripolitsa	07	354/04	264/03	141/85	0.35	7.3	Compressive
PS 3	Tripolitsa	09	188/05	092/43	283/46	0.58	6.7	Compressive
PS 4	Uppermost	13	165/15	255/01	348/73	0.9	5.3	Compressive
PS 5	Uppermost	09	018/12	279/38	122/49	0.02	5.7	Compressive
PS 6	Middle Miocene sediments	11	213/12	304/06	061/76	0.27	11.4	Compressive

n–number of fault data producing the best-fitting tensor; σ_1, σ_2, σ_3–orientations (azimuth/plunge) of principal stress axes; R – stress ratio $(\sigma_2-\sigma_3)/(\sigma_1-\sigma_3)$; A–mean slip deviation (°).

used to estimate the best-fitting stress tensor for each location. Mean slip deviation (A) between observed and predicted slips on fault planes is satisfactorily low ($\sim$ 5–11°; Table 2) for all calculated stress tensors. The graphic *P–T* axes (Turner, 1953) and the numerical dynamic analysis (Spang, 1972) methods, which were primarily proposed for calcite twinning analysis, were also applied to test the accuracy of our stress results. Basic assumptions and limitations of stress analysis, summarized by Angelier (1994), were also taken into account. The results obtained from fault-slip data analysis are listed in Table 2.

4.b. Results

All analysed carbonate samples imply a consistent subhorizontal distribution of σ_1 axes with no evidence of any tensional stress field (Fig. 10: AN 2 to AN 30). In addition, the σ_1 axes distributions reveal the existence of two main compressional trends: NNW–SSE (AN 13, 29) and NNE–SSW (AN 2, 6, 16, 23, 25, 30) (Fig. 10). It is worth noting that both trends of compression are recorded in both the Plattenkalk and the Tripolitsa units. In the two samples that yield NNW–SSE compression, the axes of maximum shortening (e_3) and compression (σ_1) are parallel to each other and subparallel ($< 20°$ deviation) to bedding dip direction (Fig. 10: inset). This calcite twinning strain fabric has been interpreted (e.g. Craddock & van der Pluijm, 1999) as indicative of strain accommodation during early layer- and transport-parallel shortening. The six samples that record NNE–SSW compression are characterized by e_3 axes that are either subhorizontal irrespective of bedding dip or consistently dip less than bedding (Fig. 10: inset). Adopting the interpretation of Harris & van der Pluijm (1998), we suggest that twinning deformation in these samples is syn- to post-folding.

Deformation at the northern flank of the Psiloritis Window is mainly accompanied by WNW-trending reverse faults as well as NNE-trending transfer faults (Fig. 10: PS 1 to PS 6). Fault-slip data analysis results reveal the existence of two compressive stress regimes: a NNW–SSE and a NNE–SSW compression. The former is recorded in two sites (PS 2, 4; Fig. 10) located in the upper tectonic units. The latter was specified using data selected from both lower (PS 1) and upper (PS 3, 5) unit rocks as well as from sediments (PS 6) of the Middle Miocene basin bordered by the Anogia Thrust (Fig. 10).

4.c. Synthesis

Results of both micro- and mesoscopic stress analyses at the northern flank of the Psiloritis Window are in very good agreement, recording two distinct compressional stress fields. The first field, which caused layer-parallel shortening in Cretan thrust sheets, trends parallel to both the L_1 orientation within the high-pressure units and the D_1 transport direction of upper units, and therefore it seems that is associated with the early deformation phase (D_1). The D_2 deformation as well as the Middle Miocene basin formation were possibly governed by the second stress field consistent with a regional compression in a NNE–SSW direction, trending normal to D_2 structures. A similar compressional trend has been also identified for the formation of late-orogenic basins throughout Crete (e.g. Meulenkamp *et al*. 1988; Kokkalas & Doutsos, 2001). Moreover, the fact that calcite twinning analysis does not record any tensional stress field confirms our interpretation that the contact between the upper and lower units was formed by compressional movements rather than by syn- or post-orogenic extension.

5. Discussion and conclusions

On the basis of kinematic and palaeostress analyses, this study distinguished two main compressional phases for the post-Eocene evolution of Cretan nappes, which resulted in the formation of NNW–SSE and NNE–SSW contraction-related structures. A third phase produced map-scale normal faults controlling the evolution of post-Middle Miocene basins of Crete. This extensional phase, which marks the onset of modern subduction of the Africa plate beneath the Aegean microplate, is extensively described in numerous studies (Doutsos & Kokkalas, 2001; Kokkalas *et al.* 2006 and references therein). In the following, we discuss the new data for the two compressional phases

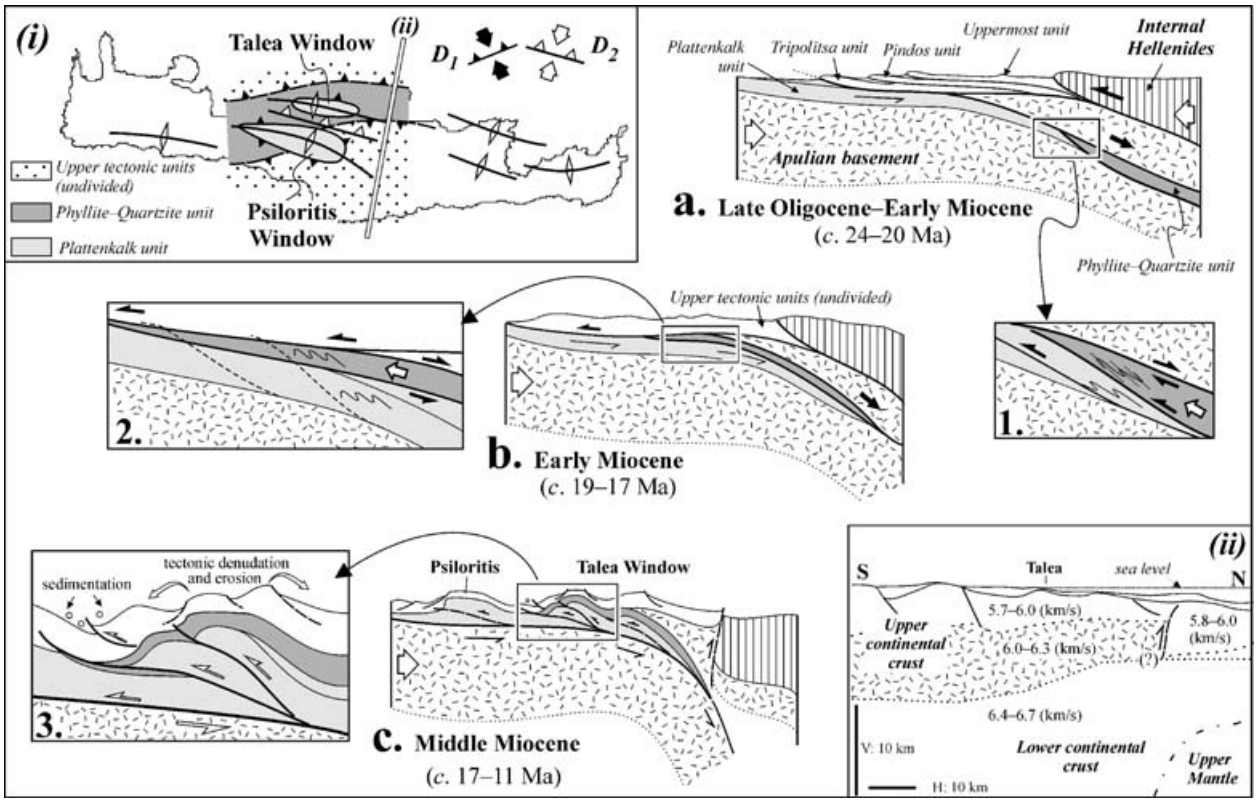

Figure 11. (a–c) Suggested geodynamic model for the orogenic evolution of central Crete along a cross-section through the Talea and Psiloritis windows. Inset (i) shows the two compressional phases controlling the post-Eocene evolution of Cretan thrust sheets as well as their associate map-scale structures. Inset (ii) shows a N-trending interpreted seismic profile across central Crete and the Cretan sea (after Bohnhoff *et al*. 2001). The steep S-dipping surface 20 km north of the Talea Window probably depicts the suture zone between the External and Internal Hellenides.

in the context of the orogenic evolution of the southern Hellenides.

5.a. Progressive underthrusting and nappe stacking

Collision of Apulia with the crust of the Internal Hellenides began in Eocene times, resulting in foreland-directed 'in-sequence' thrusting of upper tectonic units (e.g. Bonneau, 1984; Kokkalas & Doutsos, 2004). In the Early Oligocene, it seems that convergence continued further to the south along the boundary between the Tripolitsa unit and the Phyllite–Quartzite unit protolith. Therefore, the Phyllite–Quartzite unit protolith was underthrust below the Tripolitsa unit basement and was buried during Late Oligocene–Early Miocene times (*c*. 24 Ma) to a depth of 25–30 km, sufficient for high-pressure metamorphism at 8–10 kbar (Fig. 11a).

The exhumation of the Phyllite–Quartzite unit to a depth of ~10 km occurred between about 24 and 19 Ma (Thomson *et al*. 1998*a*). In the study area, this ductile stage of exhumation is recorded by a phase of penetrative deformation (D_1). Structural observations for the spatial variation in the orientation of F_1 fold axes indicate that the ductile deformation within the Phyllite–Quartzite unit was heterogeneous and was characterized by down-section increase in strain. Moreover, the increasing frequency of conjugate C′-type shear bands (late D_1 structures) towards the upper surface of the unit implies an up-section increase of the pure shear component during progressive deformation rather than a general upward decrease of the non-coaxial component. In the Peloponnese, a similar deformation pattern has been described for the Phyllite–Quartzite unit on the basis of finite strain and vorticity analyses (e.g. Xypolias & Koukouvelas, 2001; Xypolias & Kokkalas, 2006). This has been interpreted as indicative of a solid-state ductile extrusion process involving simple-shear-dominated deformation and superimposed pure shearing (see Escher & Beaumont, 1997; Xypolias, Kokkalas & Skourlis, 2003 for a similar case). By analogy, we interpret the Phyllite–Quartzite unit in central Crete as the rock body of a SSE-directed extruding shear zone. Therefore, it seems that at the Oligocene–Miocene boundary the Phyllite–Quartzite unit detached from its basement and started to extrude upward between a thrust fault at the base and the basement of the Tripolitsa unit at the top (Fig. 11: inset 1). Potentially, this tectonic extrusion process was connected with a slowdown of subduction that was probably caused by the progressive underthrusting (e.g. Ernst & Liou, 1995; Kurz, 2005)

of the less dense Plattenkalk unit and its buoyant substratum beneath the Phyllite–Quartzite unit. This underthrusting was responsible for the metamorphism and the ductile deformation of the Plattenkalk unit rocks occupying the core of the Talea Window. The relatively low deformation temperatures ($T \leq 300\,^{\circ}C$) and the absence of strong evidence for ductile deformation at the Psiloritis Window imply that the external parts of the Plattenkalk unit did not enter the subduction channel (Fig. 11b).

The end effect of the proposed extrusion process, which should have been completed before 19 Ma, was the juxtaposition of the Phyllite–Quartzite unit with the overlying upper tectonic units along a normal fault (Fig. 11: inset 2). Results of our palaeostress analysis in the area show no evidence of any crustal-scale extensional detachment between upper and lower tectonic units of central Crete, as was previously suggested (e.g. Fassoulas, 1999). A similar conclusion has been recently drawn by Campbell, Craddock & Klein (2003), also on the basis of calcite twinning analysis. Thus, it seems that the upward escape of the Phyllite–Quartzite unit is responsible for the normal fault geometry rather than north–south extension. Consequently, we suggest that extrusion of the Phyllite–Quartzite unit occurred between a lower subduction-related thrust fault and an upper 'normal fault' that operated contemporaneously in a tectonic setting without any net extension of the overall system. A similar case has been described for the Himalayas (e.g. Grujic *et al*. 1996; Vannay & Grasemann, 2001) and the Alps (e.g. Escher & Beaumont, 1997; Bucher *et al*. 2003).

5.b. Eduction of nappe stack under continuous compression

After 19 Ma the whole nappe stack was affected by a phase of NNE-directed compression, which led to the formation of large-scale thrust fault-related folds and the updoming of the Talea Window (Fig. 11c). The antiformal structure of the Psiloritis Window (Fig. 11c), as well as the roughly E-trending map-scale folds recorded throughout the island of Crete (Fig. 11: i) probably formed during this phase. Restoration of a regional cross-section (Fig. 11: inset 2) shows that SSW-directed D_2 thrusting caused an additional minimum 30 % shortening of the pre-existing nappe pile. Deformation was also penetrative at the mesoscale and is clearly recorded in the calcite fabrics. Axial-planar solution cleavage of F_2 folds indicates that early D_2 deformation took place at temperatures and depths sufficient to allow dissolution–mass transfer (at least 200 °C and 5–7 km: Holl & Anastasio, 1995). Progressive deformation produced major thrust faults accompanied by cataclastic zones, implying that unroofing of the lower high-pressure units may have resulted in decreasing temperature and confining pressure. This finding in combination with the proposed *P–T–t* path (Fig. 4a) for the Phyllite–Quartzite unit implies that brittle-stage exhumation of lower units occurred under continuous compression, which began in the time interval between 19 and 15 Ma. Orogenic compression probably lasted until the Middle–Late Miocene boundary (*c.* 11 Ma), as indicated by thrusting of the Tripolitsa unit over Serravallian sediments, as well as by contractional structures within the Middle Miocene post-orogenic basins of eastern Crete and Kos (Postma & Drinia, 1993; Kokkalas & Doutsos, 2001, 2004).

This syn-compressional exhumation of the lower high-pressure units was also synchronous with the phase of accelerated denudation of the upper units at 17–11 Ma (Thomson *et al*. 1998*b*). Therefore, the updoming of windows was accompanied by a general uplift of the area, which, however, must be isostatically compensated. Potentially, additional low-density continental material might have entered into the subduction channel during the SSW-directed thrusting and decoupling of the Cretan nappes from the pre-Alpine basement (Fig. 11: inset 3). The resistance to further underthrusting probably acted to flex the subducted slab upward and to close the subduction channel (e.g. Beaumont *et al*. 1996). The limited volume of Middle Miocene sediments suggests that the denudation of the resulting supercritical wedge on top of the slab was primarily conducted by a tectonic rather than an erosional mechanism. Progressive uplift of the area also created a gravitational potential energy, which was possibly extracted by the formation of normal faults and genetically related recumbent folds (Fig. 8: 5) at the high-altitude areas (in the sense of Gamond, 1994). These findings enable us to assume that the brittle-stage of exhumation at 17–11 Ma was accompanied by gravity sliding of the upper units (Fig. 11: inset 3). Evidence of olistoliths on top of the Middle Miocene sedimentary sequence (e.g. Postma, Fortuin & Van Wamel, 1993) also corroborate a gravity sliding process in the upper units. The closure of the subduction channel probably resulted in retro-movements at the inner portions of the belt as also occurred in Peloponnese (Xypolias & Doutsos, 2000; Doutsos *et al*. 2000). We speculate that the S-dipping surface, depicted on a seismic profile 20 km north of the Talea Window, which apparently juxtaposes crustal basement rocks on top against lower-density rocks in the footwall (Fig. 11: ii) points to major backthrusting along the suture zone between the External and Internal Hellenides.

Acknowledgements. Prof. T. Doutsos passed away while this work was in progress. Ideas presented here are the result of extensive discussion with him. We thank an anonymous reviewer for comments and Dr I. Alsop for a very careful review and valuable suggestions. We would like to thank Prof. M. A. Evans for providing us with the CSG computer program. P. X. acknowledges fruitful discussion with Prof. A. H. F Robertson on the geology of Crete. Special thanks

to Dr I. Koukouvelas and Dr S. Kokkalas for constructive comments on an early draft of the manuscript, as well as to A. Tzatzaraki for assistance in the fieldwork. V. C. was financially supported by the Tect/2003 program of the National Grants Foundation of Greece (I.K.Y.).

References

ALSOP, G. I. 1992. Progressive deformation and the rotation of contemporary fold axes in the Ballybofey Nappe, north-west Ireland. *Geological Journal* **27**, 271–83.

ALSOP, G. I., BRYSON, R. & HUTTON, D. H. W. 2001. Tectonic and kinematic evolution within mid-crustal orogenic root zones: a case study from the Caledonides of northwestern Ireland. *Geological Magazine* **138**, 193–211.

ANGELIER, J. 1994. Fault slip analysis and palaeostress reconstruction. In *Continental Deformation* (ed. P. Hancock), pp. 53–100. Oxford: Pergamon Press Ltd.

BEAUMONT, C., ELLIS, S., HAMILTON, J. & FULLSACK, P. 1996. Mechanical model for subduction-collision tectonics of Alpine-type compressional orogens. *Geology* **24**, 675–8.

BEAUMONT, C., ELLIS, S. & PFIFFNER, A. 1999. Dynamics of sediment subduction-accretion at convergent margins: Short-term models, long-term deformation, and tectonic implications. *Journal of Geophysical Research* **17**, 573–601.

BIZON, G., BONNEAU, M., LEBOULENGER, P., MATESCO, S. & THIEBAULT, F. 1976. Sur la signification et l'extension des "massifs cristallins externes" en Péloponnèse méridional et dans l'Arc égéen. *Bulletin de la Société géologique de France* **18**, 337–45.

BOHNHOFF, M., MAKRIS, J., PAPANIKOLAOU, D. & STAVRAKAKIS, G. 2001. Crustal investigation of the Hellenic subduction zone using wide aperture seismic data. *Tectonophysics* **343**, 239–62.

BONNEAU, M. 1973. Sur les affinités ioniennes des «calcaires en plaquettes» épimétamorphiques de la Crète, le charriage de la série de Gavrovo-Tripolitsa et la structure de l'arc égéen. *Comptes Rendus de l'Académie des Sciences* **277**, 2453–6.

BONNEAU, M. 1984. Correlation of the Hellenide nappes in the southeast Aegean and their tectonic reconstruction. In *The geological evolution of the Eastern Mediterranean* (eds J. E. Dixon and A. H. F. Robertson), pp. 517–27. Geological Society of London, Special Publication no. 17.

BUCHER, S., SCHMID, S. M., BOUSQUET, R. & FÜGENSCHUH, B. 2003. Late-stage deformation in a collisional orogen (Western Alps): nappe refolding, back-thrusting or normal faulting? *Terra Nova* **15**, 109–17.

BURKHARD, M. 1993. Calcite twins, their geometry, appearance and significance as stress-strain markers and indicators of tectonic regime: a review. *Journal of Structural Geology* **15**, 351–68.

CAMPBELL, H. K., CRADDOCK, J. P. & KLEIN, T. H. 2003. Calcite twinning constraints on Alpine nappe emplacement, Hellenic Arc, Crete, Greece. *Geological Society of America, Abstracts with Programs* **35**, no. 6, p. 31.

CHEMENDA, A. I., MATTE, P. & SOKOLOV, V. 1997. A model of Paleozoic obduction and exhumation of high-pressure/low-temperature rocks in the southern Urals. *Tectonophysics* **276**, 217–27.

COWAN, D. S. & SILLING, R. M. 1978. A dynamic scaled model of accretion at trenches and its implications for the tectonic evolution of subduction complexes. *Journal of Geophysical Research* **83**, 5389–96.

CRADDOCK, J. P. & VAN DER PLUIJM, B. A. 1999. Sevier-Laramide deformation of the continental interior from calcite twinning analysis, west-central North America. *Tectonophysics* **305**, 275–86.

CREUTZBURG, N., DROOGER, C.-W., MEULENKAMP, J.-E., PAPASTAMATIOU, J., SANNEMAN, W., SIEDEL, E. & TATARIS, A. 1977. *General geological map of Crete (scale 1:200 000)*. Institute of Geological and Mining Research, Athens.

DELVAUX, D. 1993. The TENSOR program for paleostress reconstruction: examples from the east African and the Baikal rift zones. *Terra Nova* **5**, 216.

DEWEY, J. F., PITMAN, W. C., RYAN, W. B. F. & BONNIN, J. 1973. Plate tectonics and the evolution of the Alpine system. *Geological Society of America Bulletin* **84**, 3137–80.

DOUTSOS, T. & KOKKALAS, S. 2001. Stress and deformation patterns in the Aegean region. *Journal of Structural Geology* **23**, 455–72.

DOUTSOS, T., KOUKOUVELAS, I., POULIMENOS, G., KOKKALAS, S., XYPOLIAS, P. & SKOURLIS, K. 2000. An exhumation model of the south Peloponnesus, Greece. *International Journal of Earth Science* **89**, 350–65.

DOUTSOS, T., PIPER, G., BORONKAY, K. & KOUKOUVELAS, I. 1993. Kinematics of the Central Hellenides. *Tectonics* **12**, 936–53.

DUNNE, W. M. & FERRILL, D. A. 1988. Blind thrust systems. *Geology* **16**, 33–6.

EPTING, M., KUDRASS, H.-R. & SCHÄFER, A. 1972. Stratigraphie et position des séries métamorphiques aux Talea Ori/Créte. *Zeitschrift der deutschen geologischen Gesellschaft* **123**, 365–70.

ERNST, W. G. 2005. Alpine and Pacific styles of Phanerozoic mountain building: subduction-zone petrogenesis of continental crust. *Terra Nova* **17**, 165–88.

ERNST, W. G. & LIOU, J. G. 1995. Contrasting plate-tectonic styles of Qinling-Dabie-Sulu and Franciscan metamorphic belts. *Geology* **23**, 353–6.

ERNST, W. G., MARUYAMA, S. & WALLIS, S. 1997. Buoyancy-driven, rapid exhumation of ultrahigh-pressure metamorphosed continental crust. *Proceedings of the National Academy of Sciences* **94**, 9532–7.

ERSLEV, E. A. & MAYBORN, K. R. 1997. Multiple geometries and modes of fault-propagation folding in the Canadian thrust belt. *Journal of Structural Geology* **19**, 321–35.

ESCHER, A. & BEAUMONT, C. 1997. Formation, burial and exhumation of basement nappes at crustal scale: a geometric model based on the Western Swiss-Italian Alps. *Journal of Structural Geology* **19**, 955–74.

EVANS, M. A. & GROSHONG, R. H. 1994. A computer program for the calcite strain-gauge technique. *Journal of Structural Geology* **16**, 277–81.

FASSOULAS, C. 1999. The structural evolution of central Crete: insight into the tectonic evolution of the south Aegean (Greece). *Journal of Geodynamics* **27**, 23–43.

FELDHOFF, R. A., LÜCKE, A. & RICHTER, D. K. 1991. Über die Diagenese-/Metamorphosebedingungen der Pindos- und Tripolitza-Serie auf der Insel Kreta (Griechenland). *Zentralblatt für Geologie und Paläontologie Teil I* **11**, 1611–22.

FORTUIN, A. R. 1978. Late Cenozoic history of eastern Crete and implications for the geology and geodynamics of the southern Aegean area. *Geologie en Mijnbouw* **57**, 451–64.

FOSSEN, H. & TIKOFF, B. 1998. Extended models of transpression and transtension, and application to tectonic settings. In *Continental Transpressional and Transtensional Tectonics* (eds R. E. Holdsworth, R. A. Strachan and J. F. Dewey), pp. 15–33. Geological Society of London, Special Publication no. 135.

GAMOND, J.-F. 1994. Normal faulting and tectonic inversion driven by gravity in a thrusting regime. *Journal of Structural Geology* **16**, 1–9.

GREILING, R. 1982. The metamorphic and structural evolution of the Phyllite-Quartzite Nappe of western Crete. *Journal of Structural Geology* **4**, 291–7.

GROSHONG, R. H. 1972. Strain calculated from twinning in calcite. *Geological Society of America Bulletin* **83**, 2025–38.

GROSHONG, R. H., TEUFEL, L. W. & GASTEIGER, C. 1984. Precision and accuracy of the calcite strain-gauge technique. *Geological Society of America Bulletin* **95**, 357–63.

GRUJIC, D., CASEY, M., DAVIDSON, C., HOLLISTER, L. S., KUNDIG, R., PAVLIS, T. & SCHMID, S. 1996. Ductile extrusion of the Higher Himalayan Crystalline in Bhutan: evidence from the quartz microfabrics. *Tectonophysics* **260**, 21–43.

HALL, R. & AUDLEY-CHARLES, M. G. 1983. The structure and regional significance of the Talea Ori, Crete. *Journal of Structural Geology* **5**, 167–79.

HANCOCK, P. L. 1985. Brittle microtectonics: principles and practice. *Journal of Structural Geology* **7**, 437–57.

HARRIS, J. H. & VAN DER PLUIJM, B. A. 1998. Relative timing of calcite twinning strain and fold-thrust belt development; Hudson Valley fold-thrust belt, New York, U.S.A. *Journal of Structural Geology* **20**, 21–31.

VAN HINSBERGEN, D. J. J. & MEULENKAMP, J. E. 2006. Neogene supradetachment basin development on Crete (Greece) during exhumation of the South Aegean core complex. *Basin Research* **18**, 103–24.

HOLL, J. E. & ANASTASIO, D. J. 1995. Cleavage development within a foreland fold and thrust belt, southern Pyrenees, Spain. *Journal of Structural Geology* **17**, 357–69.

JOLIVET, L., FACCENA, C., GOFFE, B., BUROV, E. & AGARD, P. 2003. Subduction tectonics and exhumation of high-pressure metamorphic rocks in the Mediterranean orogens. *American Journal of Science* **303**, 353–409.

JOLIVET, L., GOFFE, B., MONIE, P., TRUFFERT-LUXEY, C., PATRIAT, M. & BONNEAU, M. 1996. Miocene detachment in Crete and exhumation P-T-t paths of high-pressure metamorphic rocks. *Tectonics* **15**, 1129–53.

KATAGAS, C. 1980. Ferroglaucophane and chloritoid-bearing metapelites from the phyllite series, southem Peloponnese Greece. *Mineralogical Magazine* **43**, 975–8.

KILIAS, A., FASSOULAS, C. & MOUNTRAKIS, D. 1994. Tertiary extension of continental crust and uplift of Psiloritis metamorphic core complex in the central part of the Hellenic arc (Crete, Greece). *Geologische Rundschau* **83**, 417–30.

KOEPKE, J., SEIDEL, E. & KREUZER, H. 2002. Ophiolites on the Southern Aegean islands Crete, Karpathos and Rhodes: composition, geochronology and position within the ophiolite belts of the Eastern Mediterranean. *Lithos* **65**, 183–203.

KOKKALAS, S. & DOUTSOS, T. 2001. Strain-dependent field and plate motions in the south-east Aegean region. *Journal of Geodynamics* **32**, 311–32.

KOKKALAS, S. & DOUTSOS, T. 2004. Kinematics and strain partitioning in the southeast Hellenides (Greece). *Geological Journal* **39**, 121–40.

KOKKALAS, S., XYPOLIAS, P., KOUKOUVELAS, I. & DOUTSOS, T. 2006. Post-collisional contractional and extensional deformation in the Aegean region. In *Post-Collisional Tectonics & Magmatism in the Eastern Mediterranean Region* (eds Y. Dilek and S. Pavlides), pp. 97–123. Geological Society of America, Special Paper no. 409.

KOPP, K.-O. & OTT, E. 1977. Spezialkartierungen im Umkreis neuer Fossilfunde in Trypali- und Tripolitzakalken Westkretas. *Neues Jahrbuch für Geologie und Paläontologie Monatshefte* **1977**, 217–38.

KRAHL, J., KAUFFMANN, G., KOZUR, H., RICHTER, D., FORSTER, O. & HEINRITZI, F. 1983. Neue Daten zur Biostratigraphie and zur tektonischen Lagerung der Phyllit-Gruppe und der Trypali-Gruppe auf der Insel Kreta (Griechenland). *Geologische Rundschau* **72**, 1147–66.

KRAHL, J., RICHTER, D., FORSTER, O., KOZUR, H. & HALL, R. 1988. Zur Stellung der Talea Ori Deckenstapels (Griecheland). *Zeitschrift der deutschen geologischen Gesellschaft* **139**, 191–227.

KURZ, W. 2005. Constriction during exhumation: Evidence for eclogite microstructures. *Geology* **33**, 37–40.

KÜSTER, M. & STÖCKHERT, B. 1997. Density changes of fluid inclusions in high-pressure low-temperature metamorphic rocks from Crete: A thermobarometric approach based on the creep strength of the host minerals. *Lithos* **41**, 151–67.

LAW, R. D., SEARLE, M. P. & SIMPSON, R. L. 2004. Strain, deformation temperatures and vorticity of flow at the top of the Greater Himalayan Slab, Everest Massif, Tibet. *Journal of the Geological Society, London* **161**, 305–20.

MCCLAY, K. R. 1992. Glossary of thrust tectonics terms. In *Thrust Tectonics* (ed. K. R. McClay), pp. 419–33. London: Chapman & Hall.

MEULENKAMP, J. E., WORTEL, M. J. R., VAN WAMEL, W. A., SPAKMAN, W. & HOOGERDUYNSTRATING, E. 1988. On the Hellenic subduction zone and the geodynamic evolution of Crete since the late Middle Miocene. *Tectonophysics* **146**, 203–15.

PLATT, J. P. 1993. Exhumation of high-pressure rocks: a review of concepts and processes. *Terra Nova* **5**, 119–33.

POSTMA, G. & DRINIA, H. 1993. Architecture and sedimentary facies evolution of a marine expanding outer-arc half-graben (Crete late Miocene). *Basin Research* **5**, 103–24.

POSTMA, G., FORTUIN, A. R. & VAN WAMEL, W. A. 1993. Basin-fill patterns controlled by tectonics and climate: the Neogene 'fore-arc' basins of eastern Crete as a case history. In *Tectonic Controls and Signatures in Sedimentary Successions* (eds L. E. Frostick and R. J. Steel), pp. 335–62. International Association of Sedimentology, Special Publication no. 20.

RING, U., BRANDON, M. T., WILLET, S. D. & LISTER, G. S. 1999. Exhumation processes. In *Exhumation Processes: Normal Faulting, Ductile Flow and Erosion* (eds U. Ring, M. T. Brandon, G. S. Lister and S. D. Willet), pp. 1–27. Geological Society of London, Special Publication no. 154.

RING, U. & REISCHMANN, T. 2002. The weak and superfast Cretan detachment, Greece: exhumation at subduction

rates in extruding wedges. *Journal of the Geological Society, London* **159**, 225–8.

ROBERTSON, A. H. F., CLIFT, P. D., DEGNAN, P. J. & JONES, G. 1991. Palaeogeographic and palaeotectonic evolution of the Eastern Mediterranean Neotethys. *Palaeogeography, Palaeoclimatology, Palaeoecology* **87**, 289–343.

ROMANO, S. S., DÖRR, W. & ZULAUF, G. 2004. Cambrian granitoids in the pre-Alpine basement of Crete (Greece): Evidence from U–Pb dating of zircon. *International Journal of Earth Science* **93**, 844–59.

SEIDEL, E., KREUZER, H. & HARRE, W. 1982. A Late Oligocene/Early Miocene High Pressure Belt in the External Hellenides. *Geologisches Jahrbuch* **E23**, 165–206.

SIMPSON, C. & DE PAOR, D. G. 1993. Strain and kinematic analysis in general shear zones. *Journal of Structural Geology* **15**, 1–20.

SMITH, A. G., WOODCOCK, N. H. & NAYLOR, M. A. 1979. The structural evolution of a Mesozoic continental margin, Othris Mountains, Greece. *Journal of the Geological Society, London* **136**, 589–603.

SOUJON, A. & JACOBSHAGEN, V. 2001. Subduction of continental crust in the Hellenic arc – mid-Tertiary metamorphism of the Plattenkalk unit, Crete island, Greece. *Schriftenreihe der deutschen geologischen Gesellschaft* **14**, 201–2.

SPANG, J. H. 1972. Numerical method for dynamic analysis of calcite twin lamellae. *Geological Society of America Bulletin* **83**, 467–72.

SUPPE, J. & MEDWEDEFF, D. A. 1990. Geometry and kinematics of fault-propagation folding. *Eclogae geologicae Helvetiae* **83**, 409–54.

TEUFEL, L. W. 1980. Strain analysis of experimentally superposed deformation using calcite twin lamellae. *Tectonophysics* **65**, 291–309.

THEYE, T. & SEIDEL, E. 1991. Petrology of low-grade high pressure metapelites from the External Hellenides (Crete, Peloponnese). A case study with attention to sodic minerals. *European Journal of Mineralogy* **3**, 343–66.

THEYE, T., SEIDEL, E. & VIDAL, O. 1992. Carpholite, sudoite, and chloritoid in low-grade high-pressure metapelites from Crete and the Peloponnese. *European Journal of Mineralogy* **4**, 487–507.

THOMSON, S. N., STÖCKHERT, B., RAUCHE, H. & BRIX, M. R. 1998*a*. Thermochronology of the high-pressure metamorphic rocks of Crete, Greece: implications for the speed of tectonic processes. *Geology* **26**, 259–62.

THOMSON, S. N., STÖCKHERT, B., RAUCHE, H. & BRIX, M. R. 1998*b*. Apatite fission-track thermochronology of the uppermost tectonic unit of Crete, Greece: implications for the post-Eocene tectonic evolution of the Hellenic subduction system. In *Advances in Fission-Track Geochronology* (eds P. Van der Haute and F. De Corte) pp. 187–205. Netherlands: Kluwer Academic Publishers.

TURNER, F. J. 1953. Nature and dynamic interpretation of deformation lamellae in calcite of three marbles. *American Journal of Science* **251**, 276–98.

VANNAY, J. C. & GRASEMANN, B. 2001. Himalayan inverted metamorphism and syn-convergence extension as a consequence of a general shear extrusion. *Geological Magazine* **138**, 253–76.

WACHENDORF, H., BEST, G. & GWOSDZ, W. 1975. Geodynamische Interpretation Ostkretas. *Geologische Rundschau* **64**, 728–50.

WOODWARD, N. B., BOYER, S. E. & SUPPE, J. 1989. *Balanced geological cross-sections: An essential technique in geological research and exploration*. Washington: American Geophysical Union, 132 pp.

WOODWARD, N. B., WOJTAL, S., PAUL, J. B. & ZADINS, Z. Z. 1988. Partitioning of deformation within several external thrust zones of the Appalachian orogen. *Journal of Geology* **96**, 351–61.

XYPOLIAS, P., DÖRR, W. & ZULAUF, G. 2006. Late Carboniferous plutonism within the pre-Alpine basement of the External Hellenides (Kithira, Greece): evidence from U–Pb zircon dating. *Journal of the Geological Society, London* **163**, 539–47.

XYPOLIAS, P. & DOUTSOS, T. 2000. Kinematics of rock flow in a crustal-scale shear zone: implication for the orogenic evolution of the southwestern Hellenides. *Geological Magazine* **137**, 81–96.

XYPOLIAS, P. & KOKKALAS, S. 2006. Heterogeneous ductile deformation along a mid-crustal extruding shear zone: an example from the External Hellenides (Greece). In *Channel flow, ductile extrusion and exhumation in continental collision zones* (eds R. D. Law, M. Searle and L. Godin) pp. 497–516. Geological Society of London, Special Publication no. 268.

XYPOLIAS, P., KOKKALAS, S. & SKOURLIS, K. 2003. Upward extrusion and subsequent transpression as a possible mechanism for the exhumation of HP/LT rocks in Evia Island (Aegean Sea, Greece). *Journal of Geodynamics* **35**, 303–32.

XYPOLIAS, P. & KOUKOUVELAS, I. 2001. Kinematic vorticity and strain rate patterns associated with ductile extrusion in the Chelmos Shear zone (External Hellenides, Greece). *Tectonophysics* **338**, 59–77.

ZULAUF, G., KOWALCZYK, G., KRAHL, J., PETSCHICK, R. & SCHWANZ, S. 2002. The tectonometamorphic evolution of high-pressure low-temperature metamorphic rocks of eastern Crete, Greece: constraints from microfabrics, strain, illite crystallinity and paleodifferential stress. *Journal of Structural Geology* **24**, 1805–28.